ELSEVIER

Journal of Structural Geology 27 (2005) 1399–1412

JOURNAL OF STRUCTURAL GEOLOGY

www.elsevier.com/locate/jsg

Evaluating sand and clay models: do rheological differences matter?

Gloria Eisenstadt[a,*], Darrell Sims[b]

[a]Department of Geology, University of Texas at Arlington, 500 Yates Street, Box 19049, Arlington, TX 76019-0049, USA
[b]Center for Nuclear Waste Regulatory Analyses, Southwest Research Institute, San Antonio, TX 78238-5166, USA

Received 2 July 2004; received in revised form 3 September 2004; accepted 28 April 2005
Available online 15 July 2005

Abstract

Dry sand and wet clay are the most frequently used materials for physical modeling of brittle deformation. We present a series of experiments that shows when the two materials can be used interchangeably, document the differences in deformation patterns and discuss how best to evaluate and apply results of physical models.

Extension and shortening produce similar large-scale deformation patterns in dry sand and wet clay models, indicating that the two materials can be used interchangeably for analysis of gross deformation geometries. There are subtle deformation features that are significantly different: (1) fault propagation and fault linkage; (2) fault width, spacing and displacement; (3) extent of deformation zone; and (4) amount of folding vs. faulting. These differences are primarily due to the lower cohesion of sand and its larger grain size. If these features are of interest, the best practice would be to repeat the experiments with more than one material to ensure that rheological differences are not biasing results.

Dry sand and wet clay produce very different results in inversion models; almost all faults are reactivated in wet clay, and few, if any, are significantly reactivated in sand models. Fault reactivation is attributed to high fluid pressure along the fault zone in the wet clay, a situation that may be analogous to many rocks. Sand inversion models may be best applied to areas where most faults experience little to no reactivation, while clay models best fit areas where most pre-existing normal faults are reactivated.

Keywords: Physical models; Inversion; Extension; Shortening; Rheology; Wet clay; Sand; Reactivation

1. Introduction

Geologists have used physical modeling for over a century as a tool for understanding the development of geologic structures (e.g. Cadell, 1889; Willis, 1893). The earliest models employed a wide variety of materials in an effort to empirically replicate natural rock deformation. In 1937, methods of selecting modeling materials became more rigorous when Hubbert (1937) introduced dimensional analysis (to the English-speaking geologic community) and defined the necessary requirements for a material to be properly scaled for physical modeling.

Today, the most commonly used materials to model deformation of brittle rocks are dry sand and wet clay, but there is little agreement on their properties and suitability. While many researchers use wet clay (e.g. Cloos, 1929; Oertel, 1965; Withjack and Jamison, 1986), others maintain that clay is unsuitable for scaled modeling (Naylor et al., 1986; Mandl, 1988), suggesting that clay has a high cohesive strength that would only be appropriate for extremely high strength rocks. Additionally, critics suggest that because the effective pressure remains constant (due to the high water content of the clay), the frictional component of yield strength is independent of the confining pressure. These objections imply that wet clay would be a suitable analog only for highly cohesive rocks that deform ductility before brittle failure (Naylor et al., 1986).

There is no comparable controversy in the literature about the use of dry sand, although Mandl (1988) pointed out two problems with using sand as a modeling material. He noted that sand does not behave as an ideal frictional plastic material and so pre-faulting behavior of sand does not accurately scale to real rocks, and that the high shear dilatancy of sand creates faults whose width does not scale to actual faults.

The purpose of this study is to compare the deformation

* Corresponding author. Tel.: +1 817 272 2344; fax: +1 817 272 2628.
E-mail address: gloria_eisenstadt@yahoo.com (G. Eisenstadt).

0191-8141/$ - see front matter © 2005 Elsevier Ltd. All rights reserved.
doi:10.1016/j.jsg.2005.04.010

patterns produced by dry sand and wet clay in controlled experiments of extension, compression, and inversion. We address the following questions. (1) What are the basic rheological properties of dry sand and wet clay? (2) Do sand and clay produce similar deformation patterns under the same boundary conditions? (3) How should one best evaluate and apply modeling results to studies of actual brittle rock deformation?

2. Rheological properties of sand

While some researchers characterize granular materials such as sand as having inelastic behavior (Jaeger et al., 1996), Lohrmann et al. (2003) demonstrate that sand actually displays a more complicated rheology. Their measurements show that sand displays an elastic/frictional plastic behavior with transient strain hardening prior to failure. After failure, it exhibits strain softening until the beginning of stable sliding at constant friction. They point out that this behavior mimics that of brittle crustal rocks.

Faulting in sand is accomplished by zones of dilatancy (e.g. Reynolds, 1885; Casagrande, 1940; Mandl et al., 1977). These zones are wide, due to the relatively large size of individual sand grains. The dilatant nature of faulting in sand has no correspondence in actual rock, and the size of the fault zones and displacements in sand models do not properly scale to match real rocks (Horsfield, 1977; Mandl, 1988).

Dry sand is often selected as a material for experimental models due to ease of construction and dissection. The exact strength of sand is difficult to measure at very low values of normal stress so many researchers have linearly extrapolated from measurements made at higher values. This extrapolation yields a wide range of values of cohesive strength; 12–500 Pa (Table 1). The higher extrapolated values contradict the common observation that dry sand is virtually cohesionless, and have been the subject of discussion (Schellart, 2000; Mourgues and Cobbold, 2003).

Schellart (2000) concluded that the discrepancy between extrapolated values and observed behavior is because linear extrapolation is not a correct method for estimating the strength of sand under very low normal stresses. He showed that the failure envelope for sand, glass microspheres, and sugar at low normal stresses is convex upwards, and only approaches a straight line at higher normal stresses. Schellart measured the cohesive strength of sand as 0 Pa ($\pm$15 Pa) at zero normal stress and established that the values of cohesive strength and coefficient of internal friction are primarily dependent on rounding and sphericity and not grain size.

In contrast, Mourgues and Cobbold (2003) suggest that linear extrapolation is not the cause of erroneous large values for sand cohesion. Rather, they showed that by neglecting to account for sidewall friction in measuring sand strength, researchers have overestimated cohesion and underestimated internal friction.

Our experience comparing the behavior of dry sand and wet clay leads us to conclude that the cohesive strength of sand must be much less than wet clay but nominally greater than zero. Sand's value of cohesion is greater than zero because there may be other parameters that control sand behavior at the granular level. Sture et al. (1998) studied the behavior of sand at low stresses in the microgravity environment of space and demonstrated that the primary control on the behavior of cohesionless granular material is interparticle friction and not Coulombic forces. We observed that the behavior of sand is highly dependent on the ambient humidity, with sand appearing to have more cohesion with higher levels of humidity. This suggests that static electricity between individual sand grains may affect sand cohesion.

3. Rheological properties of wet clay

Because of the controversy over whether the cohesive strength of clay is too high to be suitable for scaled models, we measured the yield strength of the clay with several methods (Fig. 1). The wet clay (used at a density of 1.60–1.63 g/cm^3) had a cohesive strength of 60–65 Pa, measured by a controlled-stress rheometer (Appendix B). These measurements are close to an earlier published average measurement of 40 Pa (Sims, 1993) also measured by a controlled-stress rheometer, and to measurements made by an outside laboratory (Fugro-McClelland, Inc., pers. comm.) using a Fall Cone apparatus. The data definitely show that the yield strength of wet clay (in 1.58–1.82 g/cm^3 density range) is of the same order of magnitude as that of dry sand (between 0 and 100 Pa).

The data also show an increase in cohesive strength with increasing density (i.e. less water) (Fig. 1). This is in agreement with other work that shows the cohesive strength of clay is controlled primarily by water content (Terzaghi and Peck, 1948). The soil mechanics literature also documents a dramatic increase in cohesive strength of clays with increasing density (see Krynine, 1947).

Other published clay models used a variety of bulk clay densities, but do not report corresponding cohesive strength. For example, a low density value of 1.43 g/cm^3 was used by Bain and Beebe (1954), whereas Oertel (1965) reported a density of 1.75–1.80 g/cm^3. It is unknown what exact densities were used by Cloos (1929) in his clay experiments, but he noted that his most liquid clay had the consistency of sweet cream. Based on our experience, this description is consistent with a density of about 1.4–1.5 g/cm^3. Terzaghi and Peck (1948) attempted to explain the relationship between water content and cohesive strength by suggesting that cohesion in wet clays is related to the shearing strength of the adsorbed water that separate the grains and is not due to direct mechanical interaction between particles.

Table 1
Physical properties of dry sand and wet clay used in this paper and other published experiments

Modeling material	Composition and particle size (mm)	Density (g/cm^3)	Normal-fault dip	Coefficient of internal friction	Cohesion (Pa)
Dry sand (poured)[a]	Quartz $\leq$0.5	1.53	56–57	0.40–0.45	$<$300[b]
Dry sand (poured)[c]	Quartz $\leq$0.15			0.53	103[b]
Dry 'Craft' sand[c] (poured)	Quartz $\leq$0.6			0.48 (yellow and black)	$<$208 (black); 110 (yellow)[b]
Dry sand (sifted)[a]	Quartz $\leq$0.5	1.75–1.78	67–68	0.93–1.04	$<$520[b]
Dry sand (sifted)[d]	Quartz = 0.2–0.3	1.5		0.50–0.55	$<$190[b]
Dry sand (sifted)[e]	Quartz = 0.3			0.61 (unfaulted); 0.55 (faulted)	$<$300[b]
Dry sand (poured and sifted)[f]	Quartz = 0.2–0.63	1.51–1.73		0.52–0.56	37–95[b]
Dry sand[g]	Quartz = 0.125–0.4	1.6		1.18	12–72[b]
Dry sand (poured)[h]	Quartz $<$0.4	1.73	60–61	0.89	0 $\pm$ 15 (245)[b]
	Quartz $<$0.09–0.18	1.67	–	0.88	0 $\pm$ 15 (230)[b]
Wet clay[i]	Powdered kaolin, nepheline–syenite, and flint $\leq$0.1	1.63 (wet)	62 (average)		40 (average)
Wet clay[c]	Powdered kaolin, nepheline–syenite, and flint $\leq$0.1	1.57–1.82 (wet)	60–65		54–130

[a] From Krantz (1991).
[b] Linear extrapolation.
[c] This paper.
[d] From Huiqi et al. (1992).
[e] From McClay (1995) and Campbell (1994).
[f] From Lohrmann et al. (2003).
[g] From Mourgues and Cobbold (2003).
[h] From Schellart (2000).
[i] From Sims (1993).

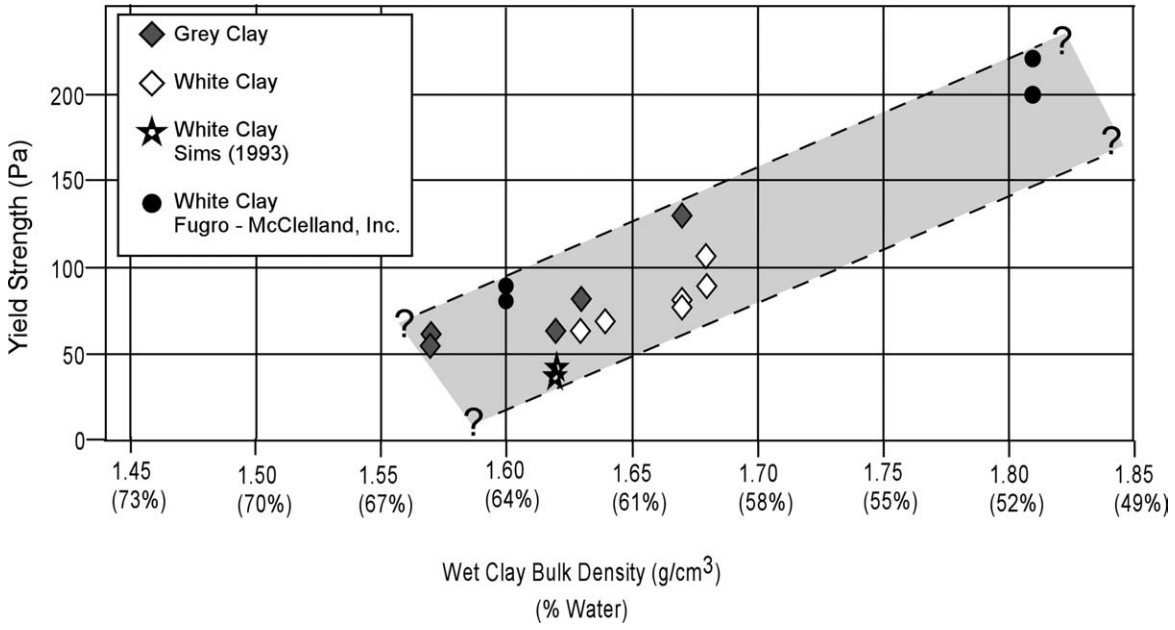

Fig. 1. Graph showing relationship between wet clay bulk density and yield strength. Values of gray and white clay and data from Sims (1993) were measured by controlled-stress rheometer, data from Fugro-McClelland, Inc., were measured by a Fall Cone apparatus. Percent water content for clay mixture was calculated using a dry bulk density of 1.68 g/cm^3. Shaded gray area shows range of values for yield strength. See Appendix B for discussion of yield strength. The same clay recipe was used for all measurements.

Because differences in deformation patterns produced in clay could also be caused by variation in strain rate, several studies have addressed the question of whether water content or strain rate is the primary control on patterns of clay deformation. All data agree that density rather than strain rate is the most important variable controlling wet clay deformation. Bain and Beebe (1954) were the first to compare the effects of varying clay density and strain rate on resulting deformation patterns. They showed that in low-density clay (1.40 g/cm^3) faults had much lower displacements, more shallow dips, and were more closely spaced than in denser clay. The only fault parameter not affected by changes in clay density was the length of fault traces. When examining the effect of varying strain rate on fault linkage, they found that the effect of decreasing displacement rate was not constant: a marked change in fault linkage occurred when the displacement rate reduced from 33 to 11 cm/h (9.2×10^{-3}–3.1×10^{-3} cm/s), but little change occurred when the displacement rate dropped from 11 to 5.7 cm/h (3.1×10^{-3}–1.6×10^{-3} cm/s). Oertel (1965) showed that the primary effects of decreasing the strain rate (by an order of magnitude) on the final deformation pattern were less acute angles between fault traces and fewer faults with greater displacement along each fault.

Other researchers have looked at the effect of varying density and/or strain rate on the nature of the faults themselves. Maltman (1987) tested clays ranging from 15 to 60% water content. He showed that deformation occurs along discrete shear zones that are 20–100 μm wide. Even low-density clays that appear to have undergone 'plastic' deformation show microscopic shear zones. Arch et al. (1988) investigated the effect of water content, strain rate, and primary fabric on shear zone geometries. They compared the geometry of shear zones over four orders of magnitude of displacement rate (10^{-4}–10^{-8} cm/s) and found no significant differences. However, they demonstrated that a change in density (20–34% water content) had a large impact on the geometry of the shear zone. In clays with low water content, the shear zones were discrete and planar, while the high water content clays had more complex and more numerous shear zones.

4. Experimental set-up

To compare the results of using dry sand vs. wet clay in physical models, we conducted a series of experiments with similar boundary conditions so that the deformation of the two materials could be compared. We chose three structural styles: extension, contraction and inversion, and repeated each with wet clay and dry sand. For all the models, layers of colored homogeneous sand or clay (4 cm total thickness) covered two overlapping thin metal plates; one attached to a fixed wall and one attached to a moveable wall (Fig. 2). The side walls were fixed.

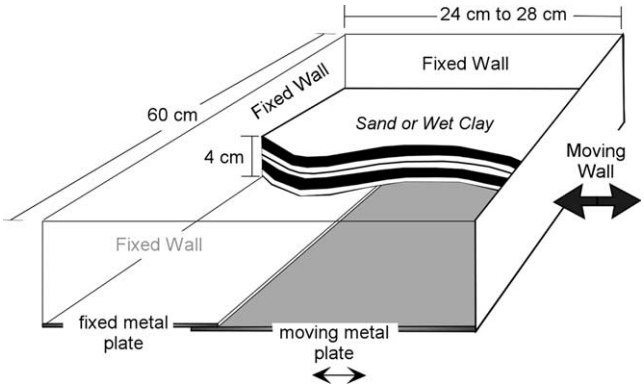

Fig. 2. Drawing of apparatus showing experimental set-up of layered sand or clay on overlapping metal plates.

The sand used in our experiments was either pure quartz sand or OK No. 1 (Table 1), which was either colored with organic dyes or mixed with a commercially dyed sand called 'Craft' sand (see Appendix A). Use of the Craft sand saved much preparation time (in dyeing the sand) but we found that the unadulterated Craft sand exhibited adhesive qualities. When a vertical cut was made in the Craft sand, the remaining face forms a slope with the uppermost 0.2–0.5 cm being vertical. When the Craft sand was mixed with 50% non-dyed OK No. 1 sand, it no longer exhibited the adhesive behavior.

The wet clay in this study was made from No. 6 tile clay (94% kaolin, 6% illite/smectitie), with minor amounts of powered feldspar and flint (Table 1). The dry clay was mixed with water to a bulk density of 1.68 g/cm^3 and colored by a local pottery supplier (the white clay was colored by adding minor amounts of minerals). The wet clay is classified as a 'sensitive' clay (Terzaghi and Peck, 1948) because it loses strength when remolded (vigorously mixed) but regains its original strength after rest.

All models were initially 60 cm long and 4 cm high. The extension models were initially 24 cm wide and were extended 4 cm (Fig. 2). The inversion models were also initially 24 cm wide, after 4 cm of extension they were shortened 4 cm. The shortening models were initially 28 cm wide, and were shortened 4 cm. The models were deformed at a rate of 1×10^{-3} cm/s (4 cm/h). We added growth layers during extension at every 1 cm of horizontal displacement. The position of the overlapping metal edge at the base determined the location of the major boundary fault in the models. This fault location remained fixed throughout the experiment, but the locations of other faults varied through time.

The sand models were wetted, sectioned, and photographed at the end of the experiments. The clay models were allowed to dry in the apparatus, then were sectioned and photographed. The clay models shrink at an average of 8% in the horizontal direction and 25% in the vertical direction, thus requiring decompaction before analysis.

5. Deformation patterns of sand vs. clay during extension

5.1. Modeling results

Final cross-sections of the extensional sand and clay experiments, cut from the center of the model, show a half-graben bounded by a master normal fault and cut by multiple antithetic faults (Fig. 3a and b). As noted by Cloos (1968) in comparable models, these sand and clay cross-sections have a similar geometry. In detail, however, two models differ. The sand model has few minor synthetic faults while the clay model has many. In the sand model, the deformed zone is narrow, there are fewer faults, each fault has more displacement, and the faults themselves are diffuse shear zones (Fig. 3a). In the clay model (Fig. 3b), many more faults are distributed over a wider zone, each fault has less displacement, and the faults are discrete, sharp boundaries. Folding also differs between the sand and clay models. Little folding occurs in the sand model, whereas most of the initial strain in the clay is accommodated by folding. The final deformation pattern of the clay model is a fault-bend fold cut by antithetic faults (Withjack et al., 1995). The same observations can be made from a comparison of clay and sand models published by Cloos (1968). His cross-section photographs show that folding accommodates a large amount of the initial deformation in the clay, and while faults initiate at the model's base, they do not propagate very quickly to the surface. In contrast, corresponding faults in his sand models appear early and quickly propagate to the surface.

Differences in deformation patterns produced by the two modeling materials are more marked if we compare the development of faults and folds throughout their deformation history (Fig. 4). The development of faults in the two materials in both cross-section and map view (only one half of the model is shown) were analyzed. Faults develop very early in sand models (at 0.25 cm), and quickly propagate upward and along strike. In contrast, through-going faults form only after 1.75 cm of displacement in the clay model. At 2 cm of extension, the deformation in the sand model (Fig. 4a) occurs primarily on a few large-displacement faults, whereas in the clay it is by folding and small-scale faulting (Fig. 4b). The faults have much greater displacement in the sand models and the deformation zone is confined to a smaller area, whereas the deformation zone is distributed over a wider area in the clay models.

There is a significant difference in how faults propagate and link in three dimensions in the two materials. There is a lack of extensive development of relay ramps in the sand

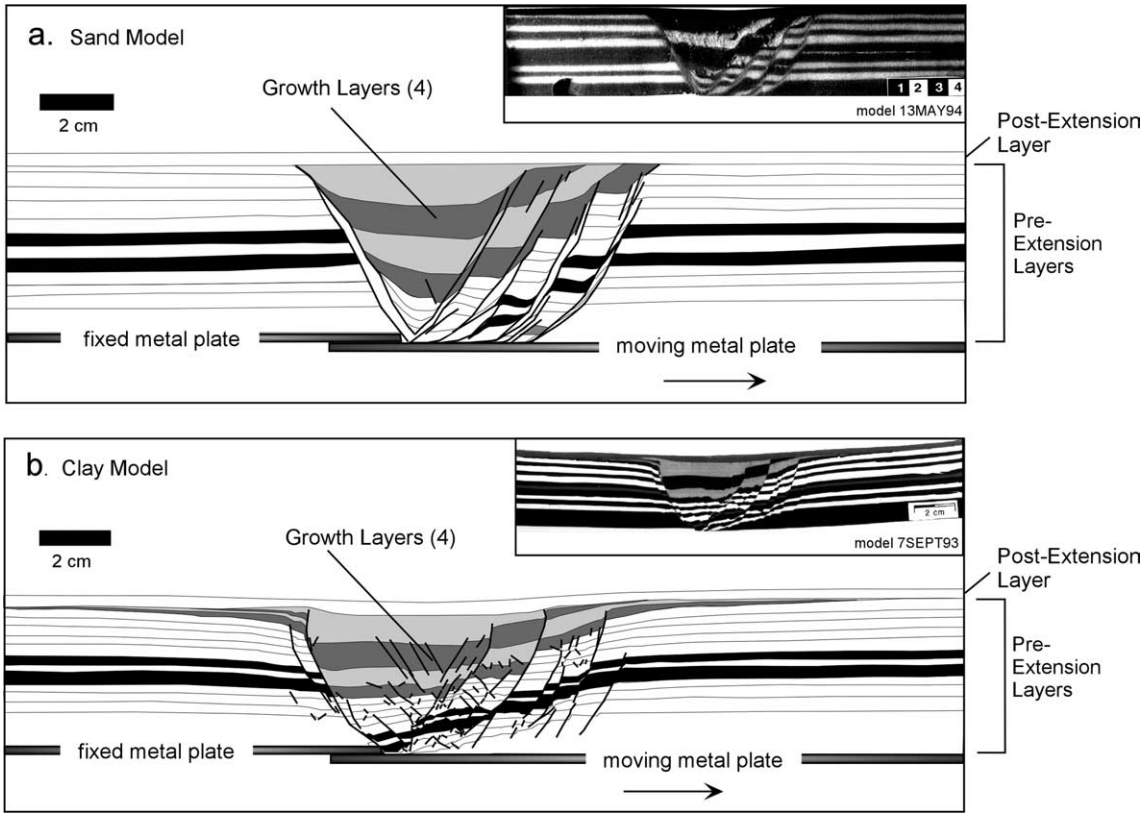

Fig. 3. Comparison of extensional models. Cross-sections were cut from the center of the model after 4 cm of extension. Insert is photograph of original model. Gray layers are growth layers added every 1 cm of extension. Clay model was decompacted to show pre-drying geometry. (a) Sand model shows half-graben bounded by large normal fault and cut by several large antithetic faults. (b) Clay model also shows half-graben bounded by large normal fault, but there are many more antithetic and synthetic faults, deforming a broader zone.

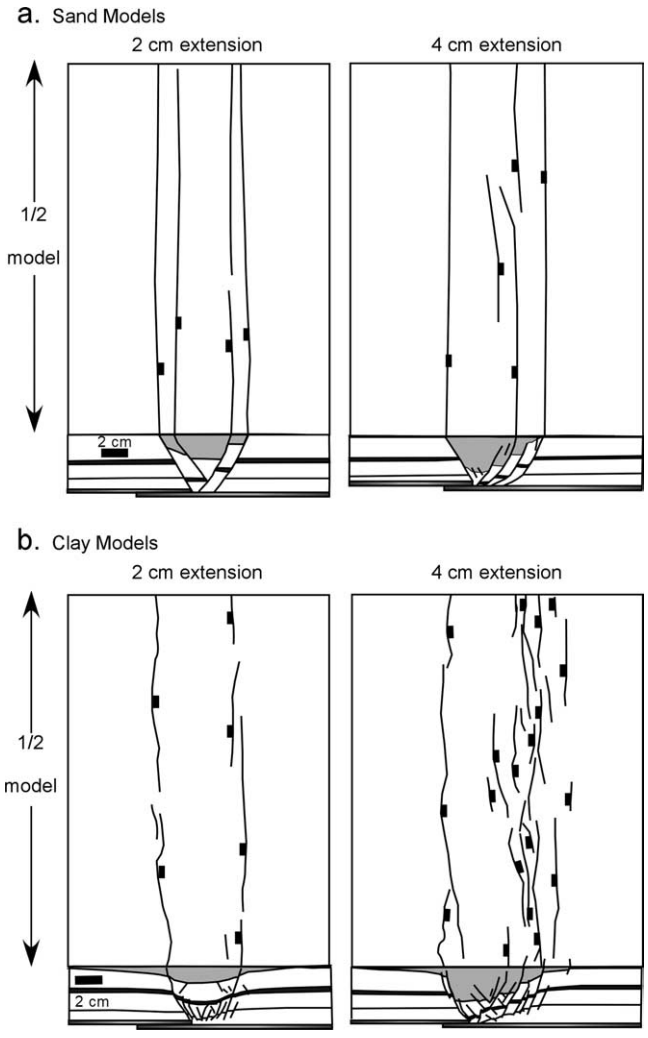

Fig. 4. Comparison of map view and cross-sections of fault development in (a) sand and (b) clay models during extension. The 2 and 4 cm diagrams are taken from separate models. Note that faults in the sand model cut the whole volume of the model at 2 cm of extension, while many in the clay model have not yet propagated to the surface. At 4 cm of extension, the sand model has fewer faults, with more linear map traces, than the clay model. The faults in the clay model form a wider zone of deformation with many relay ramps and discontinuous faults. Only one half of model is shown in map view.

model as compared with the clay. This can be clearly seen in a comparison of fault development in map view: the faults in sand are very linear, whereas the clay model has more discontinuous faults with more sinuous traces (Fig. 4a). Even at 4 cm of extension, when cross-sections of both models show a through-going master fault bounding the half-graben, these differences persist (Fig. 4b). Individual faults in the sand model have large displacements and very linear map traces, as compared with the distributed deformation and sinuous fault traces in the clay model. The sand model has few relay ramps, which are confined to a narrow band. In contrast, the relay ramps in the clay model are a complex array of many small faults distributed over a much broader deformation zone.

5.2. Discussion

The difference in faulting between dry sand and wet clay was addressed by Kautz and Sclater (1988) who compared deformation in extensional experiments. They showed that displacements on faults in sand models accounted for 70–80% of the known extension, whereas in extensional clay experiments, the slip along faults accommodated only 40–50% of the total extension. They suggested that faulting occurs over a range of scales and that the lower end of the scale is determined by grain size. Because sand has a larger grain size, it will have fewer small faults and will show more of the extension on visible faults; in clay much of the displacement occurs along very small faults.

The differences in extensional deformation patterns between dry sand and clay are important when applying modeling results to natural structures. For example, because faults propagate so quickly through sand, it is difficult to use that material to study the development and linkage of faults. In contrast, clay models show initially isolated faults that grow laterally and vertically until linked, creating complex relay zones. The development of these zones and their fault pattern is similar to those documented in natural examples (e.g. Ferrill et at., 1999; Peacock and Parfitt, 2002).

Allemand and Brun (1991) used results of a series of sand models to categorize rift basins according to width. From their experiments, they concluded that rift basin width was a function of sediment thickness and presence or absence of a ductile layer at depth. We agree with the analysis of their experimental results but caution that a direct quantitative application to real rocks may be more complicated. By comparing the same extensional models in sand and clay (Fig. 4), one can readily see that the rheology of the modeling material is an important parameter in determining the final width of the deformation zone, and that the width of the deformation zone in real rifts may not only depend on upper crustal thickness or the presence or absence of a ductile layer at depth, but also on the rheology of the overlying cover rocks themselves. Withjack and Callaway (2000) discussed this point when comparing identical sand and wet clay models of cover deformation over a basement fault. They concluded that the ductility and cohesion of the cover rocks would determine the geometry and distribution of deformation.

6. Deformation patterns in sand vs. clay during shortening

6.1. Modeling results

Cross-sections of the sand and clay shortening models, taken from the center of the models, show a similar final geometry: a flat-topped uplift bounded by conjugate thrusts dipping approximately 30–35° (Fig. 5a and b). The major difference between the two materials is that more

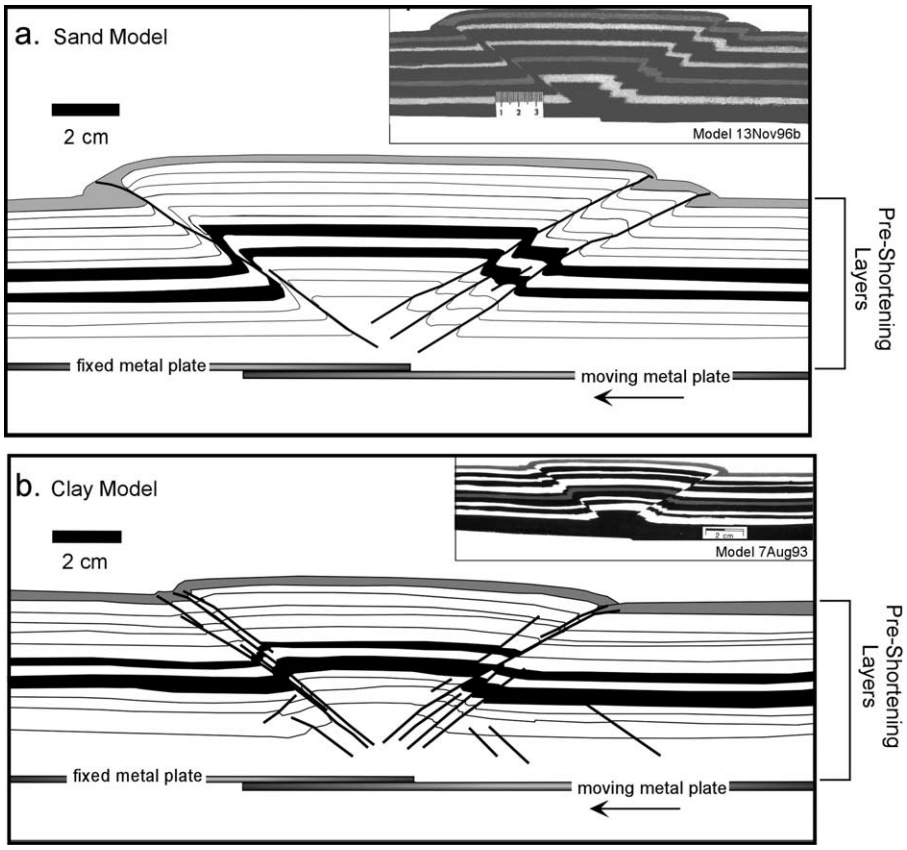

Fig. 5. Comparison of shortening models. Cross-sections from (a) sand and (b) clay models after 4 cm shortening. Cross-sections are from the center of the model. Insert is photograph of the original model. Clay model was decompacted to show pre-drying geometry.

displacement has occurred along the conjugate thrusts in the sand model, creating a wider, higher uplift. There are more subtle differences: in the sand model the main thrust, dipping toward the moving wall, is a single fault, whereas the clay model has several faults. In the sand model, the thrusts are fewer and more widely spaced, and are diffuse zones having more displacement than the thrusts in the clay models. The faults in the clay model are more numerous and closely spaced, and are discrete boundaries. The clay model also has many small incipient thrust faults dipping in both directions.

As in the extensional models, there is a difference in the development of structures (Fig. 6). At 2 cm of shortening, the sand model is already cut by conjugate thrusts while in the clay model there is little surface deformation and only a small incipient thrust in cross-section. A comparison of map patterns (Fig. 6) shows similar results to the extensional experiments. The sand model shows a simple map pattern of conjugate thrusts with little along-strike variation. In contrast, the clay model shows many small thrusts that link along strike, creating a sinuous fault zone with many small lateral ramps.

6.2. Discussion

The overall deformation geometry of the shortening models is very similar in sand and wet clay, although the detailed fault pattern, as in extension, is more complicated in the clay models. The sand model shows little-to-no lateral variation and the fault traces are very linear. In the clay model, the faults are much smaller and there is more lateral variation as faults link along strike. The shortening models are similar to the extensional models in that faults in the wet clay form much later than in the corresponding sand models.

The most interesting result in the shortening models is how much less fault displacement occurs in the clay model than in the sand. Although there are a few distributed small-scale faults, they cannot account for the difference (unlike the myriad of small-scale faults in the extensional clay model). In fact, the wet clay appears to deform differently in shortening than in extension. In the clay extension model (Fig. 3b), faults cut the whole model by 1.75 cm of displacement. In the shortening model (Fig. 5b), there is bulk thickening but little faulting for the same amount of displacement. Only at 2.4 cm of horizontal displacement do backthrusts (dipping toward the fixed wall) appear. Thus, it seems that much more strain is required to produce faulting in shortening than in extension. We suspect that shortening causes an increase in pore fluid pressure, which is not released as readily as it is during extension. The presence of high-pore fluid pressure likely delays the onset of brittle failure, and may allow appreciable ductile deformation before brittle faulting (Naylor et al., 1986).

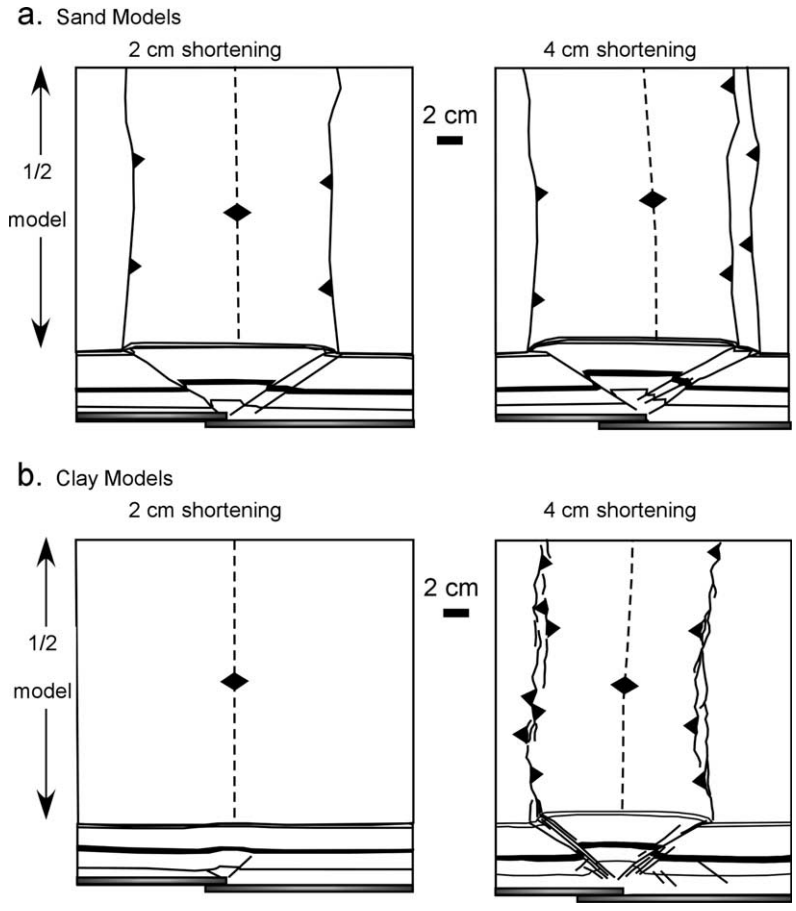

Fig. 6. Comparison of map view and cross sections of fault development in (a) sand and (b) clay models during shortening. The 2 and 4 cm diagrams are taken from separate models. Note that faults in sand model are fully formed at 2 cm of shortening while those in the clay model have not yet propagated to the surface. At 4 cm of shortening both the cross-sections and map patterns are similar, but the clay model shows multiple sinuous faults that connect with lateral ramps. Only one half of the model is shown in map view.

7. Deformation patterns of sand vs. clay during inversion

7.1. Modeling results

Cross-sections from sand and clay inversion experiments, cut from the center of the models, show dramatically different final deformation patterns (Fig. 7a and b). The sand inversion model (Fig. 7a) shows an extensional half-graben (similar to Fig. 3a) uplifted along opposing thrusts. The extensional master normal fault bounding the half-graben is barely reactivated and the extensional fault pattern is relatively undeformed as the half-graben is uplifted along the new reverse faults. In contrast, the clay cross-section (Fig. 7b) shows an uplift caused by reactivation along the original master normal fault. The original half-graben undergoes distributed deformation with reverse displacement occurring along almost all small-scale normal faults. As the half-graben is thrust along the master normal fault, secondary faults in the hanging wall are rotated into both steeper and gentler dips, and the original extensional fault-bend fold (Fig. 3b) is modified into a gentle synclinal fold (see Eisenstadt and Withjack (1995) for a full discussion of deformation features). In contrast to the sand model, where the newly formed thrusts cut the entire model thickness (Fig. 7a), the clay model (Fig. 7b) shows reverse offset along the master fault only at the uppermost growth layer. In fact, if the upper layers were removed, there would be little evidence of inversion.

7.2. Discussion

In contrast to the other experiments, deformation of wet clay and dry sand produces very different final geometries during inversion. To determine whether this difference is due to how faults are reactivated in sand vs. clay, we compared the final geometry of models that were shortened without any prior extension (Fig. 5) with models that were shortened after extension (Fig. 7). One would expect that if pre-existing faults in sand or clay were behaving as zones of weakness, they would influence the inversion geometry. This means that a model that was shortened with pre-existing faults would have a different geometry than a model that was shortened using undeformed sand or clay.

Analysis of the sand inversion experiment (Fig. 7a)

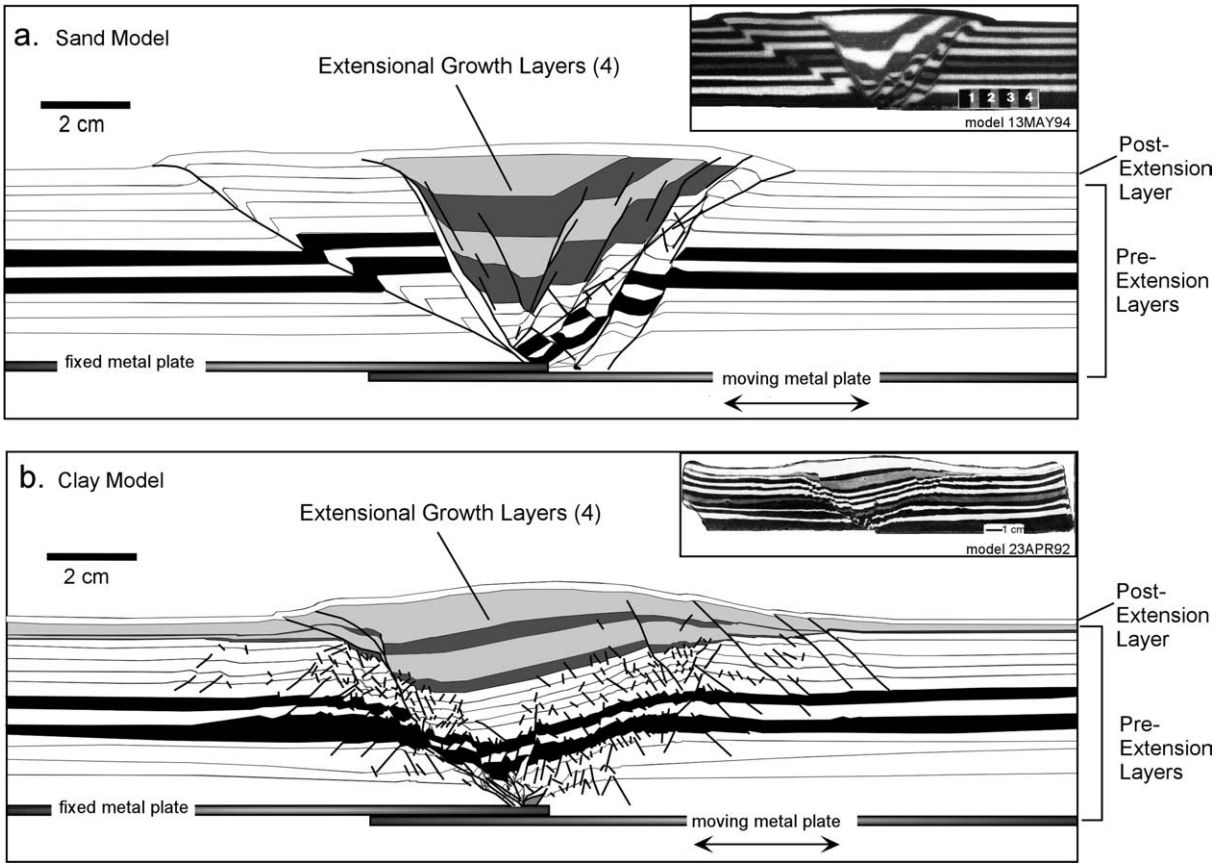

Fig. 7. Comparison of inversion models. Cross-sections were cut from the center of the model after deformation (4 cm extension followed by 4 cm shortening). Insert is photograph of the original model. Gray layers are growth layers added every 1 cm of extension. Clay model was decompacted to show pre-drying geometry. (a) Sand model shows original extensional half-graben passively uplifted along two thrust faults. (b) Clay model shows the master normal fault and many secondary faults reactivated, producing a broad uplift. Newly formed thrust faults only occur outside of the half-graben.

shows that the majority of shortening occurs along newly created conjugate thrusts, while the original normal faults are largely undeformed. This deformation is similar to that of the shortening models (without pre-existing normal faults) in both sand and clay; a pair of new conjugate thrusts bound an uplifted zone (see Figs. 5 and 8a).

The analysis is very different for the clay models; there is a striking difference between the clay inversion model (Fig. 7b) that contained pre-existing faults and the model that was shortened with no previous extension.(Fig. 5b). Large conjugate thrusts are absent in the clay inversion model, rather reverse movement is distributed amongst the pre-existing normal faults.

It is significant to note that the results of the sand inversion models are consistent with published models (Buchanan and McClay, 1991; McClay, 1991; Simmons, 1991; Krantz, 1991; Nalpas et al., 1995; Brun and Nalpas, 1996). When a sand model is inverted under various boundary conditions, sets of conjugate thrusts form that produce an uplift. The internal geometry of different sand inversion models appears complicated, but once the pattern of newly formed conjugate thrusts is recognized, the basic deformation pattern of the models is the same (Fig. 8). The pre-existing normal faults, even if they are slightly reactivated, do not significantly influence the deformation pattern. We found that regardless of differences in boundary conditions, footwall geometry, and sand composition, sand inversion models with pre-existing normal faults behave almost exactly like undeformed sand or clay.

The clay models show the other extreme of deformation: almost every fault, no matter how steeply dipping, is reactivated. The result is a zone of deformation that is distributed throughout the original half-graben. Newly formed minor thrusts are concentrated in the areas with no pre-existing normal faults. With wet clay, the pre-existing extensional faults do act as zones of weakness and exert a strong control on the resulting inversion geometry.

The ability of faults (regardless of their original dip) to reactivate in the wet clay models may be due to the high fluid pressure that exists in the clay during shortening. Experiments at Mobil Technology Company, using water-soluble coloring for the clay layers, clearly showed that colored water was expelled at the model surface along thrust fault traces during shortening. This experimental condition

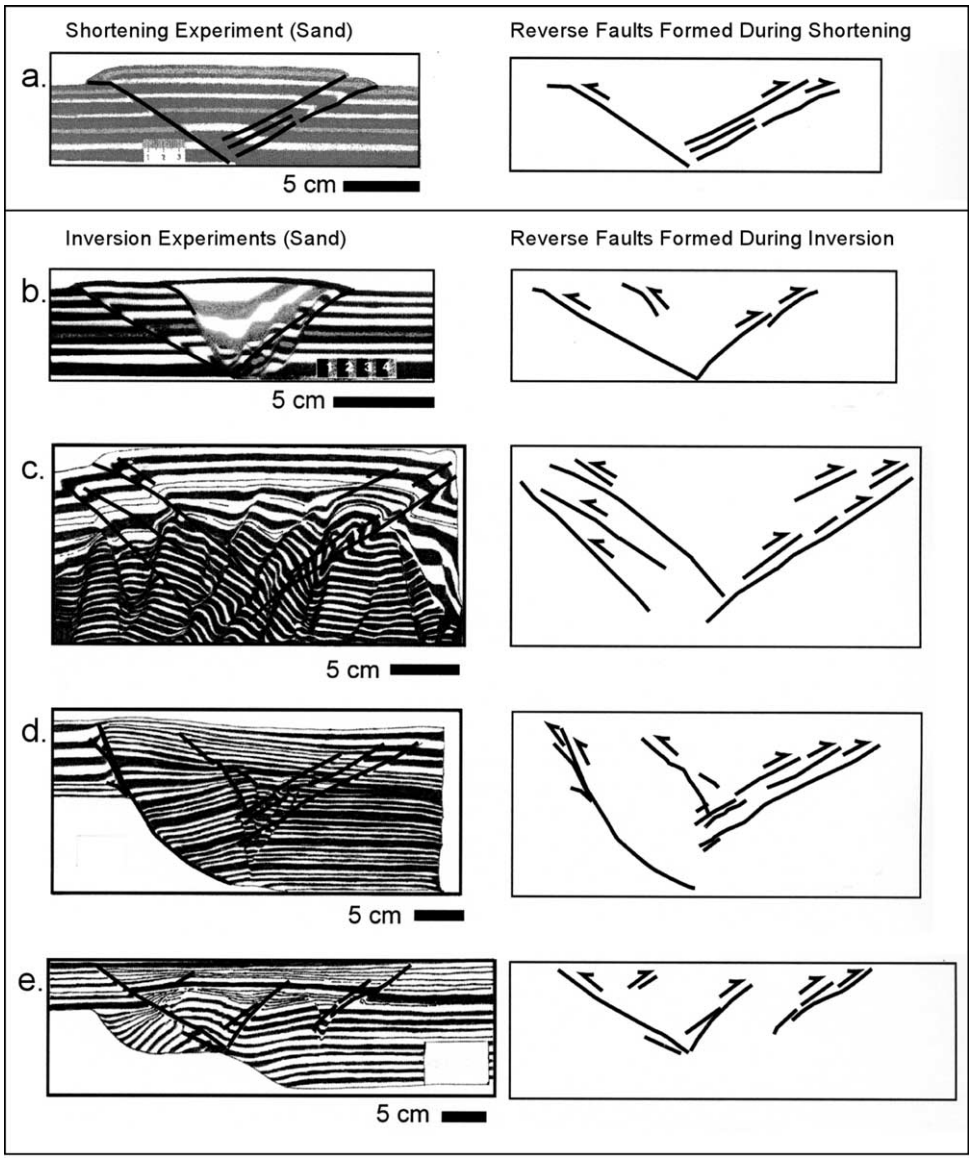

Fig. 8. Comparison of thrust patterns formed in a variety of sand experiments during shortening and inversion. Note that in dry sand, both the shortening and inversion experiments produce a conjugate thrust fault system that bypasses the original normal faults, despite variation in footwall geometry, displacement, sand composition, and experimental apparatus. (a) Shortening model (this paper) using dry sand over metal plates. Conjugate thrusts form when sand is shortened (4 cm). (b) Inversion model (this paper) using dry sand (4 cm extension, 4 cm shortening) over metal plates. (c) Inversion model using a mixture of dry sand and mica (12.5 cm extension, 7.1 cm shortening) over a horizontal detachment. Interpreted and redrawn from McClay (1989). (d) Inversion model using dry sand (7 cm extension, 8.1 cm shortening) over rigid listric footwall. Extension used a moving mylar sheet, shortening occurred with a fixed mylar sheet. Interpreted and redrawn from Buchanan and McClay (1991). (e) Inversion model using dry sand (6 cm extension, 5.5 cm shortening) over a rigid footwall with a ramp/flat geometry. Extension used a moving mylar sheet, shortening occurred with a fixed mylar sheet. Interpreted and redrawn from Simmons (1991).

may be similar to situations in real rocks where high fluid pressure enables inversion of faults that are theoretically too steep to be mechanically reactivated (Sibson, 1995).

The observation that most normal faults in sand models show little to no reactivation has been noted before, and has led researchers to a variety of conclusions about inversion structures in general. For example, Koopman et al. (1987) conducted two different sand models of inversion, both with rigid basement blocks under layered sand. They noted that the inversion was either partly or completely accommodated along new reverse faults instead of reactivating pre-existing normal faults. They concluded that the experimental models support the theoretical analysis that it becomes mechanically unfavorable to reactivate a steeply dipping normal fault as a reverse fault (Jaeger, 1960; Stearns et al., 1981; Sibson, 1985). This analysis was supported by Krantz (1991) who was only able to get fault zones in sand to reactivate by tilting the model and thereby lowering the dip of the pre-existing faults.

Nalpas et al. (1995) and Brun and Nalpas (1996) tested

the tendency of normal faults in sand to be reactivated depending on the obliquity of the shortening direction. They extended layered sand under boundary conditions similar to those in our models, and then tested different angles for the shortening direction. They showed that the pre-existing normal faults in the sand were only reactivated when the obliquity angle was lower than 45° (i.e. when there was a significant strike-slip component to the shortening). Both papers concluded that a strike-slip component of deformation was essential for fault reactivation in real rocks. We concur that there is little to no reactivation of the pre-existing normal faults in sand models without oblique shortening, but point out that this conclusion is material-dependent. Our wet clay models showed strong fault reactivation of both steep and gently dipping faults, even when the direction of later shortening is orthogonal to the trend of the normal faults.

Simmons (1991), Brun and Nalpas (1996), and McClay and Buchanan (1992) all describe similar behavior in sand during inversion experiments: little to no fault reactivation and thrust faults emanating from the tips of pre-existing normal faults. Because of the uniformity of deformation features seen in a wide variety of sand inversion models, McClay and Buchanan (1992) suggest that footwall short-cuts, out-of-the graben thrusts, and backthrusts may be diagnostic characteristics of inversion structures. In contrast, Eisenstadt and Withjack (1995) noted that these deformation features only occur in clay models after extreme amounts of shortening and that most deformation features in the clay inversion models are extremely subtle.

The fact that faults in dry sand actually show any reactivation under some circumstances has produced speculation about the nature of faulting in dry sand. Simmons (1991) noted that normal faults in the sand models have ‘no memory’. He speculated that the dilatancy that occurs within fault zones in sand disappears as the sand settles and becomes re-packed, therefore removing any mechanical contrast between the fault zones and the unfaulted sand. If true, then one would expect no reactivation, no matter what the boundary condition is. The evidence of slight reactivation of faults in sand may indicate that dilatancy along fault zones does not completely disappear (Sims et al., 1999), and therefore faults in sand have some ‘memory’ of deformation (Krantz, 1991; Lohrmann et al., 2003).

Sand and clay inversion experiments represent two end members of the behavior of real rocks. Sand models with forced motion along a rigid footwall (i.e. Fig. 8d and e) may be most analogous to inversion structures where deformation occurs only along the boundary fault. Sand models with a deformable footwall may best represent cases where there is little to no reactivation of any normal faults (Fig. 8b and c). Clay models represent the other extreme—where most pre-existing normal faults are reactivated, regardless of fault dip. In the models, this may be due to the presence of high fluid pressure along the fault zone.

8. Conclusions and application of modeling results to natural rocks

Both dry sand and wet clay are considered to behave as Mohr–Coulomb materials for the purpose of physical modeling, though neither material exhibits perfect frictional plastic behavior. Ode’ (1960) pointed out that both wet clay and dry sand deviate from idealized rock behavior in that the faulting in both materials can be stopped with the removal of applied stress, leaving the areas between faults permanently deformed; while Griffith cracks propagate close to the speed of sound and once started, cannot stop. While neither material is theoretically perfect for scaled modeling, it is remarkable how well both dry sand and wet clay reproduce deformation patterns that occur in brittle crustal rock.

By testing both materials in a series of extensional, compressional, and inversion experiments, we demonstrate that the different rheological properties of the two materials cause both subtle and significant differences in deformation patterns. The choice of which material to use in an analogue modeling depends on the deformation feature or process being investigated.

The gross deformation geometries of extensional and compressional models are similar with both sand and clay. Therefore, if large-scale geometric features are being studied, both materials will yield similar results. However, caution must be used when comparing sand and clay models because the development of the structures through time is different; through-going faults in clay do not form as quickly as they do in sand.

Rheological differences between dry sand and wet clay do cause subtle but important small-scale differences in deformation during extension and shortening. Dry sand has lower cohesion and a larger grain size than wet clay. These factors create the following differences:

1. *Fault propagation rate and fault linkage*. Faults develop and link rapidly in dry sand while initiating and propagating slowly in wet clay. The slower fault linkage in wet clay, coupled with more numerous and sinuous faults, creates more relay ramps in extension and more lateral ramps in compression.
2. *Fault width, spacing, and displacement*. The larger grain size of dry sand is responsible for wider fault zones in sand models. Because dry sand is weaker than wet clay, faults form more quickly in sand. There is more displacement along individual faults, and fewer faults are formed in sand than in wet clay.
3. *Extent of deformation zone*. Because faults form and propagate so rapidly in sand, deformation is quickly accommodated along those faults, creating a limited deformed volume. Much of the early faulting in clay is microscopic in scale, and is manifested as distributed deformation. The slower rate of fault propagation in clay means that more deformation is distributed along small

faults before they finally link and form through-going faults.

4. *Amount of folding vs. faulting*. The low cohesion of sand precludes any significant folding; most strain is accommodated by faulting. In contrast, wet clay deforms by both faulting and folding.

If physical modeling is being used to study the above deformation features, it may be necessary to repeat experiments with both dry sand and wet clay. This precaution will prevent properties specific to either sand or clay from biasing the results.

We found that fault reactivation is the deformation feature most sensitive to rheological differences. There is a large difference in both large-scale and detailed inversion geometries between dry sand and wet clay models. Faults in sand are barely reactivated. There are some thrusts that emanate from the tips of pre-existing normal faults, but most shortening is accommodated along newly formed sets of conjugate thrusts. The geometry of inverted sand models closely resembles that of sand models without pre-existing normal faults.

In contrast, almost all pre-existing extensional faults in wet clay behave as zones of weakness and show reactivation during inversion. The shortening is distributed throughout the original extensional half-graben; small thrusts appear primarily in areas of the model that contained no pre-existing normal faults. Our experiments suggest that the high water content of wet clay (Fig. 1) may have an effect on its behavior during shortening and inversion. During shortening, the high pore fluid pressure seems to delay fault formation, so that less displacement is observed along faults than in corresponding extensional experiments. During inversion, the high fluid pressure appears to facilitate fault reactivation along pre-existing extensional faults regardless of dip or orientation.

Many conclusions about the geometry and kinematics of inversion structures have been derived from sand models and may not apply to all natural examples. Clay models, in contrast to sand, show that steeply dipping faults can be significantly reactivated in pure orthogonal shortening; strike-slip displacement is not necessary. Deformation patterns in clay models suggest that footwall shortcuts, backthrusts, and out-of-graben thrusts (common features of sand inversion models) may not be ubiquitous features of actual inversion structures. Instead, in the clay models, inversion is distributed throughout the original extensional half-graben along many small-scale normal faults. The nature of the small-scale deformation in the clay models means that such features, if occurring with inversion in natural rocks, would be very difficult to image on seismic data. We suggest that clay models are most applicable to inversion structures with fault zones substantially weaker than the host rock; either because of high fluid pressure along fault zones (Sibson, 1995) or because the fault gouge itself is weaker than the host rock (Stearns et al., 1981).

Acknowledgements

We thank the management of Mobil Technology Company for their support in this research, and ExxonMobil Corporation for permission to publish the results. Selena Dixon and Charlie Wall provided excellent technical assistance. An interest in the rheological differences between sand and clay grew out of work and discussions with Martha Withjack and Bruno Vendeville, whose suggestions greatly improved an earlier version of this paper. We also thank Jo Lohrmann, David Ferrill, Larry McKague, and an anonymous reviewer for their thorough reviews.

Appendix A. Pre-dyed Sand

Pre-dyed silica craft sand is available from Activa Products, Inc. The sand needs to be sieved to remove coarser fractions and mixed with 50% (by volume) non-dyed sand. It is currently available in 22 colors.

Activa Products, Inc., P.O. Box 472, Westford, MA 01886, USA. +1 508 692 9300. www.activa-products.com

Appendix B. Measuring cohesive strength of wet clay

The cohesive strength of clay was determined by measurements using a CarrieMed™ CSL 100 controlled stress rheometer with a parallel plate configuration. The clay sample is placed between two horizontal circular plates. The bottom plate is lowered to facilitate sample loading and then raised to a pre-determined height, but it does not rotate. The 4 cm diameter upper plate is fixed to a vertical shaft that is supported by an air bearing. Torque is imparted to the shaft via induction, and the torque translates to a recorded shearing stress proportional to the area of the plate contacting the sample. Supported by the air bearing, the vertical stress exerted upon the sample via the upper plate is virtually zero. For the clay measurements, the distance between the plates is 1500 μm, more than 10 times the diameter of the largest particle (100 μm) within the sample. The rheometer surfaces in contact with the sample are machined stainless steel and while not polished are relatively smooth. Slippage was observed in some tests, identified by carefully lowering the bottom plate and examining the clay surface after each test. Results with evidence of slip between the plate and sample were discarded.

Sample thickness, when loaded between the upper and lower plates, is so small that vertical stress imparted by sample mass is assumed to be negligible. The sample is placed between the plates and allowed to equilibrate for 10 min before the test begins. Equilibration allows elastic strains imparted during sample loading to relax (Sims, 1993). After equilibration, shear stress is increased linearly

from zero and shear strain and stress recorded. When non-recoverable shear strain is greater than zero, the corresponding shear stress (yield stress) is recorded.

Failure was observed to occur along a discrete surface invariably in the uppermost portion of the sample. In some tests, vertical markers were applied to the clay when exposed at the edge of the parallel plate system. Markers were applied by touching the clay with a thin knife blade, taking care not to touch the rheometer plates. This produced a very narrow ridge in the clay that was oriented perpendicular to the rheometer plates. Visual comparison using a small machinist's square as reference before and after testing showed no detectable shearing of the markers, except at the discrete failure plane.

The failure plane in the clay sample was observed as parallel with the rheometer plates. Because the upper plate is supported by an air bearing, and because the failure plate occurred near, but not at, the contact between the sample and the upper plate, the normal stress across the failure plane was assumed to be zero. Yield stress of the clay is recorded at the amount of shear stress required to induce non-recoverable shear strain in the test sample. Frictional or Mohr–Coulomb materials are said to have cohesive strength if a plane with zero normal stress will support some shear stress without displacement. From simple observation, it is clear that frictional failure models such as Mohr–Coulomb do not adequately describe the material properties of the clay mix used in these experiments. In the case of the clay tests reported here, clay yield stress is similar to cohesive strength in that it is a measure of resistance to shearing along a plane with zero normal stress. For convenience, we refer to the clay yield stress as cohesive strength.

References

Allemand, P., Brun, J.-P., 1991. Width of continental rifts and rheological layering of the lithosphere. Tectonophysics 188, 63–69.

Arch, J., Maltman, A.J., Knipe, R.J., 1988. Shear-zone geometries in experimentally deformed clays: the influence of water content, strain rate and primary fabric. Journal of Structural Geology 10, 91–99.

Bain, G.W., Beebe, J.H., 1954. Scale model reproduction of tension faults. American Journal of Science 252, 745–754.

Brun, J.-P., Nalpas, T., 1996. Graben inversion in nature and experiments. Tectonics 15 (2), 677–687.

Buchanan, P., McClay, K.R., 1991. Sandbox models of inverted listric and planar fault systems. Tectonophysics 188, 97–115.

Cadell, H.M., 1889. Experimental researches in mountain building. Transactions Royal Society of Edinburgh Pt. 1, 337–357.

Campbell, I., 1994. 2D and 3D Extension and Inversion of Convex-up Fault Systems. MSc Thesis. Royal Holloway, University of London, 127pp.

Casagrande, A., 1940. Characteristics of cohesionless soils affecting the stability of slopes and earth fills. Contributions to Soil Mechanics vol. n1925–1940, 257–276.

Cloos, H., 1929. Kunstliche Gebirge. Natur und Museum 59, 225–243.

Cloos, E., 1968. Experimental analysis of Gulf Coast fracture patterns. American Association of Petroleum Geologists Bulletin 52 (3), 420–444.

Eisenstadt, G., Withjack, M.O., 1995. Estimating inversion: results from clay models. In: Buchanan, J.G., Buchanan, P.G. (Eds.), Basin Inversion Geological Society Special Publication, 88, pp. 119–136.

Ferrill, D.A., Stamatakos, J.A., Sims, D., 1999. Normal fault corrugation: implications for growth and seismicity of active normal faults. Journal of Structural Geology 21, 1027–1038.

Horsfield, W., 1977. An experimental approach to basement-controlled faulting. Geologie en Mijnbouw 56 (4), 363–370.

Hubbert, M.K., 1937. Theory of scale models as applied to the study of geologic structures. Geological Society of America Bulletin 48, 1459–1520.

Huiqi, L., McClay, K.R., Powell, D., 1992. Physical models of thrust wedges. In: McClay, K.R. (Ed.), Thrust Tectonics. Chapman & Hall, London, pp. 71–81.

Jaeger, J.C., 1960. Shear failure of anisotropic rocks. Geologic Magazine 97, 65–72.

Jaeger, H.M., Nagel, S.R., Behringer, R.P., 1996. The physics of granular materials. Physics Today, 32–38.

Kautz, S.A., Sclater, J.G., 1988. Internal deformation in clay models of extension by block faulting. Tectonics 7 (4), 823–832.

Koopman, A., Speksnijder, A., Horsfield, W.T., 1987. Sandbox model studies of inversion tectonics. Tectonophysics 137, 379–388.

Krantz, R.W., 1991. Measurements of friction coefficients and cohesion for faulting and fault reactivation in laboratory models using sand and sand mixtures. Tectonophysics 188 (1/2), 203–207.

Krynine, D.P., 1947. Soil Mechanics. Its Principal and Structural Applications. McGraw-Hill, New York. 511pp.

Lohrmann, J., Kukowski, N., Adam, J., Oncken, O., 2003. The impact of analogue material properties on the geometry, kinematics, and dynamics of convergent sand wedges. Journal of Structural Geology 25, 1691–1711.

Maltman, A., 1987. Shear zones in argillaceous sediments—an experimental study. In: Jones, M.E., Preston, R.M. (Eds.), Deformation of Sediments and Sedimentary Rocks Geological Society Special Publication, 29, pp. 77–87.

Mandl, G., 1988. Mechanics of Tectonic Faulting. Elsevier, Amsterdam. 407pp.

Mandl, G., de Jong, N.J., Maltha, A., 1977. Shear zones in granular material. Rock Mechanics 9, 95–144.

McClay, K.R., 1989. Analogue models of inversion tectonics. In: Cooper, M.A., Williams, G.D. (Eds.), Inversion Tectonics Geological Society Special Publication, 44, pp. 41–59.

McClay, K.R., 1995. Geometries and kinematics of inverted fault systems. In: Buchanan, J.G., Buchanan, P.G. (Eds.), Basin Inversion Geological Society Special Publication, 88, pp. 97–118.

McClay, K.R., Buchanan, P.G., 1992. Thrust faults in inverted extensional basins. In: McClay, K.R. (Ed.), Thrust Tectonics. Chapman & Hall, London, pp. 93–104.

Mourgues, R., Cobbold, P.R., 2003. Some tectonic consequences of fluid overpressures and seepage forces as demonstrated by sandbox modeling. Tectonophysics 376, 75–97.

Nalpas, T., Douaran, S., Le, S., Brun, J.-P., Unternehr, P., Richert, J.-P., 1995. Inversion of the Broad Fourteens Basin (offshore Netherlands), a small-scale model investigation. Sedimentary Geology 95, 237–250.

Naylor, M.A., Mandl, G., Sijpesteijn, C.H.K., 1986. Fault geometries in basement-induced wrench faulting under initial stress states. Journal of Structural Geology 8 (7), 737–752.

Ode', H., 1960. Faulting as a velocity discontinuity in plastic deformation. In: Griggs, D., Handin, J. (Eds.), Rock Deformation: A Symposium Geological Society of America Memoir, 79, pp. 293–321.

Oertel, G., 1965. The mechanism of faulting in clay experiments. Tectonophysics 221, 325–344.

Peacock, D.C.P., Parfitt, E.A., 2002. Active relay ramps and normal fault propagation on Kilauea Volcano, Hawaii. Journal of Structural Geology 24, 729–742.

Reynolds, O., 1885. On the dilatancy of media composed of rigid particles in contact. Philosophical Magazine 20, 46.

Schellart, W.P., 2000. Shear test results for cohesion and friction coefficients for different granular materials: scaling implications for their usage in analogue modeling. Tectonophysics 324, 1–16.

Sibson, R.H., 1985. A note on fault reactivation. Journal of Structural Geology 7, 751–754.

Sibson, R.H., 1995. Selective fault reactivation during basin inversion: potential for fluid redistribution through fault-valve action. In: Buchanan, J.G., Buchanan, P.G. (Eds.), Basin Inversion Geological Society Special Publication, 88, pp. 3–19.

Simmons, M., 1991. An experimental study of the geometries and kinematics of inversion and growth structures. MSc Thesis. Royal Holloway and Bedford New College, University of London, 113pp.

Sims, D., 1993. The rheology of clay: a modeling material for geologic structures (abs.). EOS Transactions. American Geophysical Union 74, 569.

Sims, D., Ferrill, D.A., Stamatakos, J.A., 1999. Role of ductile decollement in the development of pull-apart basins: experimental results and natural examples. Journal of Structural Geology 21, 533–554.

Stearns, D.W., Couples, G.D., Jamison, W.R., Morse, J.D., 1981. Understanding faulting in the shallow crust: contributions of selected experimental and theoretical studies. In: Carter, N.L., Friedman, M., Logan, J.M., Stearns, D.W. (Eds.), Mechanical Behaviors of Crustal Rocks, The Handin Volume Geophysical Monograph, 24. American Geophysical Union, pp. 215–229.

Sture, S., Costes, N.C., Batiste, S.N., Lankton, M.R., AlShibli, K.A., Jeremic, B., Swanson, R.A., Frank, M., 1998. Mechanics of granular materials at low effective stresses. Journal of Aerospace Engineering 11, 67–72.

Terzaghi, K., Peck, R.B., 1948. Soil Mechanics in Engineering Practice. Wiley, New York.

Willis, B., 1893. The Mechanics of Appalachian Structure: US Geological Survey. 13th Annual Report, Part 2, 211–281.

Withjack, M.O., Callaway, S., 2000. Active normal faulting beneath a salt layer: an experimental study of deformation in the cover sequence. American Association of Petroleum Geologists Bulletin 84, 627–651.

Withjack, M.O., Jamison, W.R., 1986. Deformation produced by oblique rifting. Tectonophysics 126, 99–124.

Withjack, M.O., Islam, Q.T., La Pointe, P.R., 1995. Normal faults and their hanging-wall deformation; an experimental study. American Association of Petroleum Geologists Bulletin 79, 1–18.